FIRE AND MATERIALS
Fire Mater. 2016; **40**:80–88
Published online 29 October 2014 in Wiley Online Library (wileyonlinelibrary.com). DOI: 10.1002/fam.2270

Experimental study of the burning behavior of *n*-heptane pool fires at high altitude

Zhihui Zhou[1,4], Wei Yao[2], Xiaokang Hu[3], Richard Yuen[4] and Jian Wang[1,*,†]

[1]*State Key Laboratory of Fire Science, University of Science and Technology of China, Hefei 230027, China*
[2]*LHD, Institute of Mechanics, Chinese Academy of Sciences, Beijing 100190, China*
[3]*Shanghai Institute of Satellite Engineering, Shanghai, 201107, China*
[4]*Department of Civil and Architectural Engineering, City University of Hong Kong, Kowloon, Hong Kong*

SUMMARY

The same configured calorimeters were built in Hefei (99.8 kPa) and Lhasa (66.5 kPa), respectively. Four sizes of round pans with diameters of 10, 15, 20, and 25 cm were adopted to study the effect of high altitude on the burning behavior of liquid pool fires. Analysis on the burning rate obtained in this study and in the literature at different altitudes indicates that pressure fire modeling performs better than radiation fire modeling in correlating the burning intensity (burning rate per unit area) with pressure and pool diameter for cases under low ambient pressure. The study also shows that heat release rate and combustion efficiency decrease at higher altitude. For medium pool fires, the burning intensity and heat release rate are proportional to $D^{5/2}$, thus the combustion efficiency being independent on pool sizes but decreases at higher altitude by a factor approximate to the pressure ratio. Copyright © 2014 John Wiley & Sons, Ltd.

Received 8 August 2013; Revised 21 March 2014; Accepted 21 August 2014

KEY WORDS: high altitude; *n*-heptane pool fire; burning intensity; heat release rate; combustion efficiency

1. INTRODUCTION

Burning rate and total heat release rate are two critical parameters to characterize the burning behavior of a fire load in fire hazard analysis [1, 2], and liquid pool fires are usually selected for research purpose because of its simple diffusion flame structure and relatively stable burning process [3–5]. An early systematic study on the burning rate was conducted by Blinov and Khudiakov [6]; based on those results, Hottel [7] pointed out that conservation of energy can be applied to pool fires, and two basic radiatively and convectively dominated burning regimes can be divided. The studies [6, 7] also indicated that the conductive heat transfer is the most critical factor in determining the burning rate for the diameter of pool being less than 7 cm [6–8]. Fang *et al*. [9] analyzed the variation of burning rate with pressure based on Hottel's theory and concluded that the dominated heat transfer mechanism transits from conduction to convection and radiation as the pool diameter increases from 4 to 33 cm. Thus, the heat transfer mechanism should be also taken into account in predicting the burning behavior of pool fires at high altitude.

Two main modeling approaches were developed by De Ris [10, 11] to scale the mass burning rate with the pool dimension and the ambient pressure, which was initiated to large-scale fires to small laboratory fires for the convenience of measurement and analysis. Although these modelings are mostly established under high pressure, they have been also proved to be suitable for the cases of the reduced

*Correspondence to: Jian Wang, State Key Laboratory of Fire Science, University of Science and Technology of China, Hefei 230027, China.
†E-mail: wangj@ustc.edu.cn

pressure (or at high altitude) [12–14]. Pressure modeling, based on the assumption of the identical Grashof number (Gr) and Froude number (Fr), had been critically tested for convection-dominated fires [15–17], which indicated that if the pool diameters meet the requirement $D \sim P^{-2/3}$, the dimensionless burning intensity (burning rate per unit area) can be scaled with the product of pressure-squared times length-cubed as $m'' D \sim P^2 D^3$ for pool fires with diameter D [10]. Radiation modeling was established upon the hypothesis that the burning intensity remains constant by holding the product of pressure-squared times length $P^2 D$ invariant [11], which is based on the two assumptions that soot radiation is dominant and a second-order pressure dependence of soot formation rate, as both have been derived in International Standard for Fire Tests—Full-Scale Room Test for Surface Products and Kanury [18, 19].

In this paper, the burning rate and heat release rate of round *n*-heptane pool fires with four different sizes were measured at a high-altitude city Lhasa (66.5 kpa) and a sea-level city Hefei (99.8 kpa) to examine the pressure effect on the burning behavior of pool fires. The correlation between mass burning rate and pressure for pool fires of different sizes was analyzed, and the combustion efficiency at high altitude estimated from the total heat release rate was discussed in the following texts.

2. EXPERIMENTAL DESIGN

2.1. Fire test platform

The same configured calorimeters shown in Figure 1 (a) were installed in Lhasa and Hefei, respectively. Smaller exhaust systems were designed for this study purpose as 40% of that in ISO 9705 [18]. Similarly, the calorimeter mainly consists of an exhaust hood, pipeline, fan, transducer, gas analyzer, and flow measurement equipment as schematically shown in Figure 1 (b). The hood used to collect the exhaust gas has a vent of 0.36×0.36 m at the top and 1.2×1.2 m at the bottom. The diameter and length of the exhaust pipe are 0.16 and 3 m, respectively. Guide vanes were mounted at the ends of the exhaust pipe to ensure that flow into the gas analyzer section is uniform. The measurement section of exhaust gas is 0.6 m in length. Kane KM9106 Quintox portable gas analyzer is used to record the temperature rise and CO, CO_2, and O_2 concentration. The flow velocity is measured by a Kano 6162 high-temperature anemometer. Brackets are fixed below the hood to support the entire apparatus. The half bottom keeps opening, while glasses are installed at its upper half to stabilize the pool fire from the disturbance of surrounding air flow.

2.2. Experimental configuration

The experimental configuration is listed in Table I. The pool fire tests were conducted in two altitudes, that is, 50 m in Hefei and 3650 m in Lhasa. The fire tests were conducted using round fuel pans with

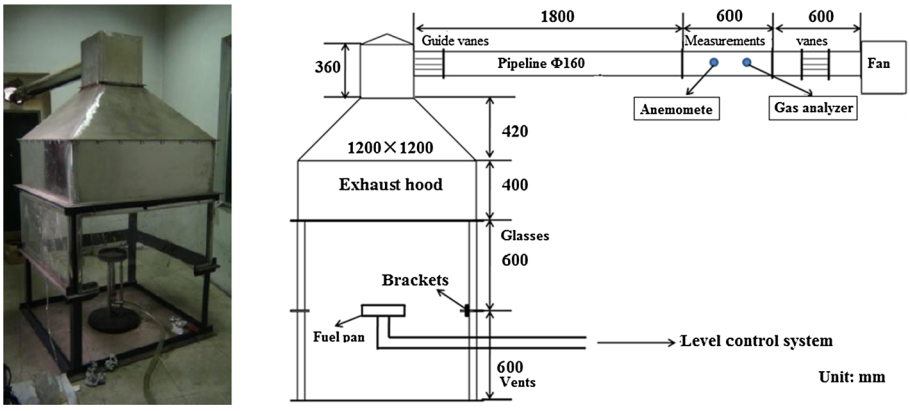

(a) (b)

Figure 1. Configuration of the experimental calorimeter.

DOI: 10.1002/fam

Table I. The configuration of the experimental cases and conditions.

Case		Pool diameter (m)	Flow velocity (m/s)	Air humidity (%)	Ambient temperature (°C)
Hefei	Case A	0.10	4.5	63	8.5
	Case B	0.15	4.5	62	8.5
	Case C	0.20	6	57	10.7
	Case D	0.25	7	60	9.9
Lhasa	Case A	0.10	4.5	56	19.4
	Case B	0.15	4.5	56	21.7
	Case C	0.20	6	50	22.6
	Case D	0.25	7	48	23.5

different sizes, that is, 10, 15, 20, and 25 cm. The tested fuel is liquid *n*-heptane with industrial purity above 99% (impurity contents: volatile $\leq 0.05\%$, water $\leq 0.05\%$, and unsaturated compounds in $Br^+ \leq 0.032\%$). In the tests, the pan is located just under the exhaust hood and 0.6 m above the floor. Figure 2 shows the self-leveling reservoir designed according to the one used by De Ris [11] to maintain the liquid rim level in the burning pan, in which case the pool can be assumed to simulate an infinite depth of fuel. The electronic scale with resolution of 0.1 g is placed beneath the self-leveling reservoir to record the mass loss of fuel during the burning process. Each test was repeated at least three times to ensure reproducibility of results.

To ensure that all the products of combustion can be pumped into the pipeline, rather than escaping from the edge of hood, the fan should provide sufficient ventilation rate, that is, the exhaust rate must be much larger than the mass entrainment rate $\dot{m}_{fan} >> \dot{m}_{ent}$, where $\dot{m}_{fan} = \rho_s \pi D_{pipe}^2 v/4$, ρ_s—gas density, v—gas velocity, and D_{pipe}—the pipeline diameter. The entrained mass flow rate is given by $\dot{m}_{ent} = 0.0056\dot{Q}_c$ [1], where $\dot{Q}_c$ is the convective heat release rate, and $\dot{Q}_c \approx 0.7\dot{Q}$ under the prevailing assumption. The total heat release rate is calculated by $\dot{Q} = \chi \dot{m} H_c$, where the heat of combustion of *n*-heptane (H_c) is 48 kJ/g, $\dot{m}$—the burning rate, and χ—the combustion efficiency usually less than the unity. The maximum mass entrainment rate $\dot{m}_{ent,\max}$ can be obtained by the further assumption of $\chi = 1$. Table II lists the used exhaust rates for different fire loads. Note that although the exhaust rate $\dot{m}$ *fan* is not very larger than the maximum mass entrainment in case D, its value still exceeded $\dot{m}_{ent,\max}$ about 10%, which indicated that enough oxygen had been supplied for supporting the fuel combustion process.

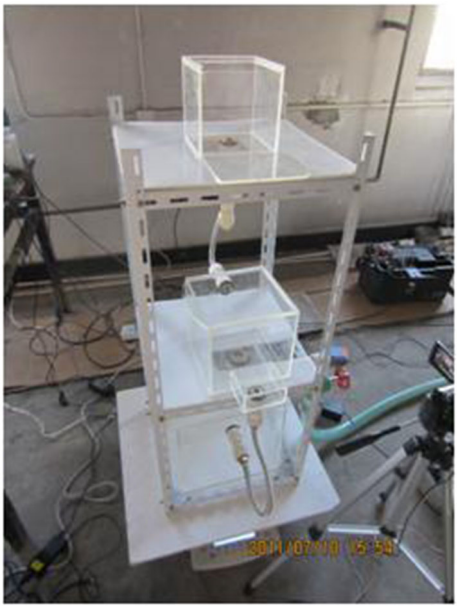

Figure 2. Self-leveling reservoir used to maintain the liquid rim level.

DOI: 10.1002/fam

Table II. Mass flow rates of entrainment and smoke exhaust.

	Hefei (g/s)			Lhasa (g/s)		
	m	$\dot{m}_{ent,\,max}$	$\dot{m}$ *fan*	$\dot{m}$	$\dot{m}_{ent,\,max}$	$\dot{m}$ *fan*
Case A	0.085	0.016	0.117	0.065	0.012	0.073
Case B	0.215	0.040	0.117	0.147	0.027	0.073
Case C	0.432	0.081	0.156	0.277	0.052	0.098
Case D	0.745	0.140	0.182	0.547	0.103	0.114

3. RESULTS AND DISCUSSION

3.1. Burning process

Figure 3 shows the burning rate curves of pool fires with different diameters in Hefei and Lhasa. The mass burning rates were derived from mass loss curves recorded by the electronic scale. It is clear that the burning rate in Hefei is much higher than that in Lhasa. The mass burning rate gradually increases from the start because of the increase in fuel temperature preheated by the flame heat feedback. A quasi-steady stage can be generally distinguished in cases of 10–20 cm as 150 s after the ignition till 500 s (when bubbles were observed to emerge, rising from the pan bottom), and then, the burning rate increases rapidly because of boiling by the accumulation of thermal feedback, whereas the starting time for the 25-cm pool shows a little delay of 50 s, and the quasi-steady burning can be record as a shorter value during time from 200 to 450 s, which can be also approximately identified by the sharp changes in the time derivative of the burning rates. Thus, for a unified analysis, the mean burning intensity is then calculated from the data for the quasi-steady burning stage to characterize the burning behavior of pool fires at the two altitudes.

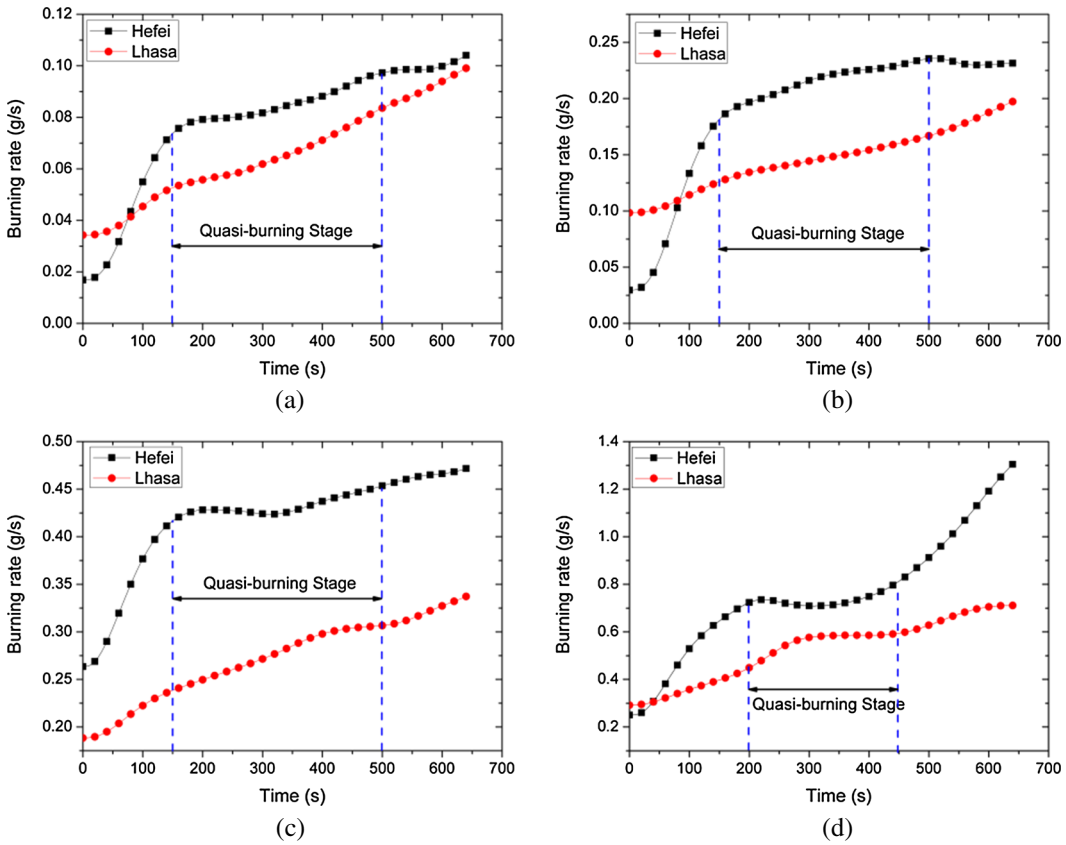

Figure 3. Mass burning rate of pool fires with different diameters: (a) 10, (b) 15, (c) 20, and (d) 25 cm.

DOI: 10.1002/fam

3.1. Scale modeling of mass burning rate

3.2.1. Pressure modeling. To model the fluid mechanics of fires, one must reproduce both the Fr ($\mathrm{Fr} = (\rho_\infty u^2)/(\Delta\rho g l)$) and the Reynolds number ($\mathrm{Re} = \rho_\infty u l/\mu$), which can be actually combined in the form of a rearranged Gr.

$$Gr = \frac{g\rho l^3 \Delta\rho}{\mu^2} = \left(\Delta\rho g l/\rho u^2\right)(\rho u l/\mu)^2 \tag{1}$$

where μ—the dynamic viscosity, g—the gravity acceleration, and $\Delta\rho/\rho$ are all independent of pressure, while $\rho \sim P$. Thus,

$$\rho^2 l^3 = constant \tag{2}$$

Then, many experiments based on the assumption in pressure modeling had been critically tested for convection-dominated fires [15–17] or in the hypothesis that fire radiation, if important, should be proportional to the rate of combustion, where $\dot{m}'' \sim P^{2/3}$ [10]. It indicated that if the characteristic length met the requirement of the constant $\rho^2 l^3$, the dimensionless burning intensity (burning rate per unit area) can be scaled with a power function of Gr as $\dot{m}'' l/\mu \sim fcn(Gr)$. In addition, De Ris pointed out that, for the pool fires, the characteristic length l is usually represented by the pool diameter D [19]. The simplified formula can be expressed as the following, which is also consistent with the experimental results from the tests of Yao *et al*. [20] on cardboard box fires:

$$\dot{m}'' D \sim fcn\left(P^2 D^3\right) \tag{3}$$

3.2.2. Radiation modeling. Radiation modeling is established upon the hypothesis that the burning intensity remains constant by holding the product of pressure-squared times length invariant as expressed in Eqn 4 [11],

$$\rho^2 l = constant \tag{4}$$

The theory of radiation fire modeling develops from the basic understanding of pressure effects on soot formation, which is pointed out as that soot radiation is dominant and a second-order pressure dependence of soot formation rate, as both are consistent in Yao *et al*. and Yao *et al*. [21, 22].

Meanwhile, soot radiation is considered as the primary source of the flame heat flux, where the burning rate is determined by flame radiative heat feedback. De Ris *et al*. [11] found that, if the proposed radiation modeling scheme is valid, the mass burning intensity should be correlated by the product $P^2 D$ (note that the characteristic length is replaced by the pool diameter); then

$$\dot{m}'' \sim fcn\left(P^2 D\right) \tag{5}$$

3.2.2. Assessment of fire modelings. The previous two fire modelings are critically assessed according to the analysis of the experimental data reported by Fang *et al*. and Tu *et al*. [9,23] and the results in our study, as shown in Figures 4 and Figure 5.

Figure 4 shows the burning intensity scaled by pressure modeling, where the measured data points are generally concentrated on the linear fitting in the logarithmic coordinates, with a fitting power of 0.45 that is, $\dot{m}'' D \sim \left(P^2 D^3\right)^{0.45}$, and the adjusted coefficient of determination of 0.984, 0.968, and 0.987 for ethanol, heptane, and the present work, respectively, although the fitting power is a litter larger than the theoretical value 1/3, which may be caused by the underestimated change in flame radiation. Kanury [19] predicted that the flame heat feedback is predominantly convective in the range of $108 < \mathrm{Gr} < 1010$; the fitted result indicates that the application of pressure fire modeling could extend to the range of $106 < \mathrm{Gr} < 109$ (where $\mathrm{Gr} = 1.457 \times 10 \times \mathrm{P^2D^3}$ [15]), which should be available for *n*-heptane pool fires at both normal and high altitude.

The plotting in Figure 5 indicates that data points scaled by radiation modeling are scattered, and the data trend for satisfying fitting is not as good as in the pressure modeling with the adjusted coefficient

DOI: 10.1002/fam

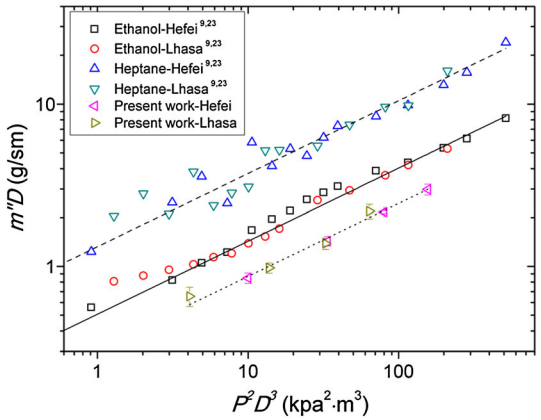

Figure 4. Burning intensity scaled by pressure modeling.

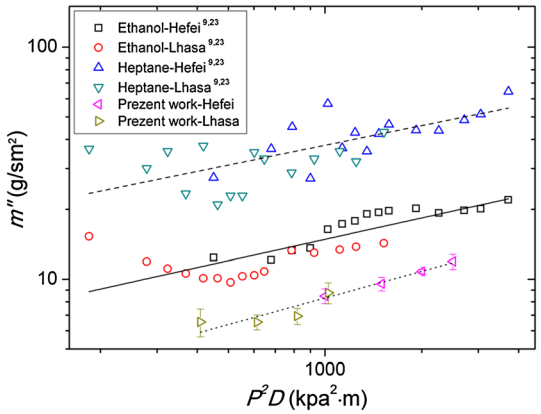

Figure 5. Burning intensity scaled by radiation modeling.

of determination of 0.692, 0.505, and 0.945 for ethanol, heptane, and the present work, respectively. Radiation fire modeling is built by emphasizing the role of radiation (mainly from soot) in determining the burning rate. However, it seems that the flame convection plays a significant role for pool fires of moderate sizes [1,8], especially for the cases with the decreasing soot fraction aroused by the lower ambient pressure, and previous studies also reported that the burning rate is proportional to $P^{2/3}$ [23, 24].

Generally, pressure fire modeling seems more available for the pool fires under low pressure, especially for that the pool size is limited and not very large, that is, flame radiative heat transfer is not dominated. It can be attributed to that (1) ethanol and *n*-heptane belong to weakly sooting and moderately sooting fuel [8], (2) for pools with the diameter of 7–30 cm, the convective heat term predominates flame heat feedback; soot radiation is not the major part in determining the burning rate [8,25], and (3) soot formation reduces with the decreasing of pressure in a second order [22].

3.2. Heat release rate and combustion efficiency

In 1917, Thornton found that for a large number of organic liquids and gases, an almost constant net amount of heat is released per unit mass of oxygen consumed for complete combustion [26]. Huggett validated the constant net heat release per unit mass of oxygen consumed for organic solids and obtained an average value of 13.1 kJ/g ± 5% for the constant [27]. Based on the theory of constant heat release per unit mass of oxygen consumed, the basic method of obtaining heat release rate by measuring the oxygen consumption was established by DiNenno and Parker [1,28] and extended with the consideration of air pressure influence as

DOI: 10.1002/fam

$$\dot{Q} = \left[E\phi - (E_{CO} - E)\frac{1-\phi}{2}\frac{X_{CO}^{A^e}}{X_{O_2}^{A^e}}\right] \cdot \frac{\dot{m}_e}{1+\phi(\alpha-1)}\frac{M_{O_2}}{M_a}\left(1 - X_{H_2O}^{a}\right)X_{O_2}^{A^a} \tag{6}$$

with oxygen depletion factor

$$\phi = \frac{X_{O_2}^{A^a}\left(1 - X_{CO_2}^{A^e} - X_{CO}^{A^e}\right) - X_{O_2}^{A^e}\left(1 - X_{CO_2}^{A^a}\right)}{\left(1 - X_{O_2}^{A^e} - X_{CO_2}^{A^e} - X_{CO}^{A^e}\right)X_{O_2}^{A^a}} \tag{7}$$

where the heat release per mass unit of oxygen consumed ($E = 13.1$ kJ/g) and that for the conversion from CO to CO_2 ($E_{CO} = 17.6$ kJ/g) are independent of air pressure; $\alpha = 1.105$ is the volumetric expansion factor; $M_{O_2} = 28$ g/mol and $M_a = 29$ g/mol are molecular weights of oxygen and air; $X_{O_2}^{A^e}$, $X_{CO_2}^{A^e}$, and $X_{CO}^{A^e}$ are measured mole fractions of O_2, CO_2, and CO in the exhaust flow; $X_{O_2}^{A^a}$, $X_{CO_2}^{A^a}$, and $X_{CO}^{A^a}$ are mole fractions of O_2, CO_2, and CO in the air; $X_{H_2O}^{a}$ is the mole fraction of water vapor in the air calculated from its vapor pressure; and $\dot{m}_e$ is mass exhaust rate calculated from the exhaust velocity v, the gas temperature T, and the cross-section area of pipeline A.

The mean heat release rate at the stage of quasi-steady burning is calculated by Equation 6, with the measurements of exhaust gas concentration variation. It indicates that heat release rate decreases with the increasing altitude, partly because of the decreasing burning rate, as plotted in Figure 6.

Figure 6 shows the averaged heat release rate and burning rate scaled by 5/2 power of pool diameter for the repeated experiments with the uncertainty of the tests that is also presented by error bars. Mulholland *et al.* [29] suggested that $\dot{Q} \sim D^{5/2}$ for $D < 1$ m, correlated from the measurements of heat release rate for *n*-heptane and crude oil pool fires. It indicates that this conclusion can also be applied at high altitudes. For pool fires in moderate size $0.1\text{ m} < D < 1$ m, the measurement of crude oil fires by Koseki *et al.* [30] suggested that $\dot{m}'' \sim D^{1/2}$, which was also validated in the ethanol and *n*-heptane pool fire tests in Lhasa by Tu *et al.* [14]. Then, the mass burning rate can be scaled with the pool diameter by $\dot{m} = \pi \dot{m}'' D^2/4 \sim D^{5/2}$.

Finally, it is easy to obtain the conclusion that combustion efficiency ($\chi = \dot{Q}/\dot{m}H_c$) is a constant just determined by ambient pressure, being independent of pool diameter for moderate pool fires. The combustion efficiency values of quasi-steady burning stage measured in current experiments are drawn in Figure 7. It indicates that χ deceases with the increasing altitude (reduce pressure), and being generally invariant with the pool diameter except for that in the case of a 10-cm pan in Hefei, which could be explained by the diameter being close to the lower limit of moderate pool fires dominated by the convection term [6], and the significantly higher combustion efficiency is also observed. The mean χ of pool fires in Hefei and Lhasa is $77.3 \pm 4.3\%$ and $49.7 \pm 0.8\%$. It is found that $\chi(\text{Lhasa})/\chi(\text{Hefei}) \approx 0.64$, which is approximately equal to the ratio of ambient pressure at the

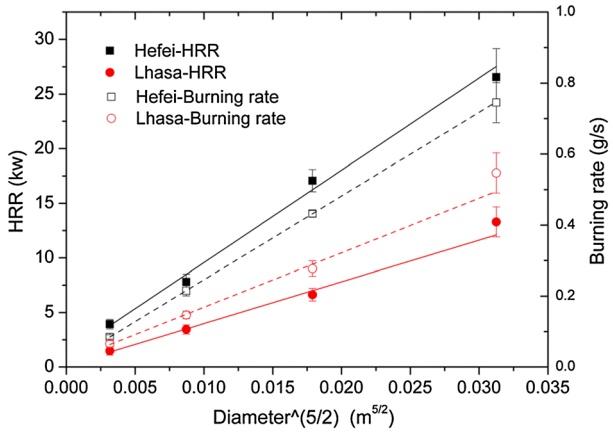

Figure 6. Heat release rate and burning rate correlated with $D^{5/2}$.

DOI: 10.1002/fam

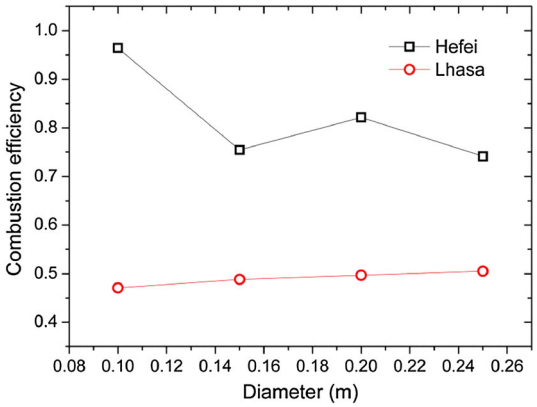

Figure 7. Combustion efficiency of pool fires with different diameters at two altitudes.

two altitudes. It may be aroused from 'fuel-rich' combustion [31] caused by the decreasing air concentration. The tested combustion efficiency χ at high altitude is extremely low but still above the critical value of 0.35, which would lead to the flame extinguishment [31].

Moreover, lots of experiments about the raised pressure effects on major heat release chemistry have been performed [32–34], although the cases for the decreasing pressure are still unknown, for example, Carriere *et al*. [32] proposed that the reaction pathways of ethylene combustion should change when affected by the ambient pressure. It indicated that C_2H_4 is mainly consumed by abstraction in the low-pressure flame, while abstraction (mainly by OH instead of H) competes with H addition that forms C_2H_5 in the high-pressure system. Thus, the low air pressure influence on combustion chemical reaction is essential and needs further study.

4. CONCLUSION

The mass burning rate, gas concentrations, and heat release rate were measured for *n*-heptane pool fires of different sizes at high altitude (Lhasa, 3650 m) and a sea-level altitude (Hefei, 50 m), and the main conclusions are given as follows:

1. The comparison shows that pressure fire modeling performs better than radiation fire modeling in correlating the burning intensity with the pressure and pool diameter, which is fitted by the burning data at high altitude measured in this study and available in the literature as a scaling function $\dot{m}'' D \propto \left(P^2 D^3\right)^{0.45}$. The applicable range of pressure modeling is extended into $106 < \mathrm{Gr} < 109$.
2. For convection-dominated medium pool fires ($0.1\ \mathrm{m} < D < 1\ \mathrm{m}$), both the burning intensity and the total heat release rate fit the scale relation $\dot{m}'', \dot{Q} \propto D^{5/2}$, which was validated by the total heat release rate estimated from the consumption of three major gas species oxygen, CO, and CO_2. The scale relation implies constant combustion efficiency independent of pan sizes, which was confirmed by the current burning data, and the combustion efficiency decreases at higher altitude by a factor approximate to the pressure ratio.

ACKNOWLEDGEMENTS

The work described in this paper was supported by the National Natural Science Foundation of China (No: 51376172) and a grant from the Research Grant Council of the Hong Kong Special Administrative Region (Project No. CityU 122612). The authors deeply appreciate the support.

REFERENCES

1. DiNenno PJ. SFPE Handbook of Fire Protection Engineering. National Fire Protection Association: Quincy, Massachusetts. 2002.
2. Babrauskas V, Peacock RD. Heat release rate: the single most important variable in fire hazard. *Fire Safety Journal* 1992; **18**(3):255–272.

DOI: 10.1002/fam

3. Blinov V, Khudyakov G. Diffusion burning of liquids. DTIC Document, 1961.
4. Hall A. Pool Burning: a Review. DTIC Document, 1972.
5. Yin JS, Yao W, Liu QY, Zhou ZH, Wu N, Zhang H, Lin CH, Wu T, Meier OC. Experimental study of n-Heptane pool fire behavior in an altitude chamber. *International Journal of Heat and Mass Transfer* 2013; **62**(1):543–552.
6. Blinov VI, Khudiakov GN. Certain Laws Governing Diffusive Burning of Liquids. *Academiia Nauk, SSSR Doklady* 1957; **113**:1094–1098.
7. Hottel HC. Review of Certain Laws Governing Diffusive Burning of Liquids. *Fire Research Abstracts and Teviews* 1959; **1**:41–44.
8. Hamins A, Fischer SJ, Kashiwagi T, Klassen ME, Gore JP. Heat Feedback to the Fuel Surface in Pool Fires. *Combustion Science and Technology* 1994; **97**(1-3):37–62.
9. Fang J, Tu R, Guan J, Wang J, Zhang Y. Influence of low air pressure on combustion characteristics and flame pulsation frequency of pool fires. *Fuel* 2011; **90**(8):2760–2766.
10. De Ris J, Kanury AM, Yuen MC. Pressure modeling of fires. *Proceedings of the Combustion Institute* 1973; **14**(1):1033–1044.
11. De Ris J, Wu PK, Heskestad G. Radiation fire modeling. *Proceedings of the Combustion Institute* 2000; **28**(2):2751–2759.
12. Wieser D, Jauch P, Willi U. The Influence of High Altitude on Fire Detector Test Fires. *Fire Safety Journal* 1997; **29**(2):195–204.
13. Jun F, Yu C-Y, Ran T, Qiao L-F, Zhang Y-M, Wang J-J. The influence of low atmospheric pressure on carbon monoxide of n-heptane pool fires. *Journal of Hazardous Materials* 2008; **154**(1-3):476–483.
14. Tu R, Fang J, Zhang Y-M, Zhang J, Zeng Y. Effects of low air pressure on radiation-controlled rectangular ethanol and n-heptane pool fires. *Proceedings of the Combustion Institute* 2012; **34**(2):2591–2598, doi: 10.1016/j.proci.2012.06.036.
15. Alpert RL. Pressure modeling of fires controlled by radiation. *Proceedings of the Combustion Institute* 1977; **16**(1):1489–1500.
16. Alpert RL. Pressure modeling of transient crib fires. *Combustion Science and Technology* 1977; **15**(1-2):11–20.
17. Alpert RL. Pressure Modeling of Fire Growth in Enclosures. *Fireline* 1978; **5**(1):7–7.
18. International Standard for Fire Tests-Full-Scale Room Test for Surface Products. International Organization for Standardization: Geneva, Switzerland, 1993.
19. Kanury AM. Modeling of pool fires with a variety of polymers. *Proceedings of the Combustion Institute* 1975; **15**(1):193–202.
20. Yao W, Hu X, Rong J, Wang J, Zhang H. Experimental study of large-scale fire behavior under low pressure at high altitude. *Journal of Fire Sciences* 2013; **31**(4):481–494.
21. Yao W, Zhang J, Nadjai A, Beji T, Delichatsios MA. A global soot model developed for fires: validation in laminar flames and application in turbulent pool fires. *Fire Safety Journal* 2011; **46**(7):371–387.
22. Yao W, Zhang J, Nadjai A, Beji T, Delichatsios M. Development and Validation of a Global Soot Model in Turbulent Jet Flames. *Combustion Science and Technology* 2012; **184**(5):717–733.
23. Tu R, Fang J, Zhang YM, Zhang J, Zeng Y. Effects of low air pressure on radiation-controlled rectangular ethanol and n-heptane pool fires. *Proceedings of the Combustion Institute* 2012; **34**(2):2591–2598.
24. Niu Y, He Y, Hu X, Zhou D, Lin CH, Yin J, Yao W, Wang J. Experimental study of burning rates of cardboard box fires near sea level and at high altitude. *Proceedings of the Combustion Institute* 2012; **34**(2):2565–2573.
25. Yao W, Nadjai A, Delichatsios M, Zhang J. A global soot model for fires: application in turbulent pool fires. Sixth International Seminar on fire and explosion hazards. Leeds, UK, 2010.
26. Thornton W. The relation of oxygen to the heat of combustion of organic compounds. *Philosophical Magazine Series* 1917; 33:196–203.
27. Huggett C. Estimation of rate of heat release by means of oxygen consumption measurements. *Fire and Materials* 1980; **4**(2):61–65.
28. Parker WJ. Calculations of the Heat Release Rate by Oxygen Consumption for Various Applications. *Journal of Fire Sciences* 1984; **2**(5):380–395.
29. Mulholland GW, Henzel V, Babrauskas V. The effect of scale on smoke emission. *Proceedings of the second International Symposium on Fire Safety Science*, Hemisphere, New York, 1988; 347–357.
30. Koseki H, Mulholland GW. The Effect of Diameter on the Burning of Crude Oil Pool Fires. *Fire Technology* 1991; **27**(1):54–65.
31. Tewarson A. Combustion efficiency and its radiative component. *Fire Safety Journal* 2004; **39**(2):131–141.
32. Carriere T, Westmoreland PR, Kazakov A, Stein YS, Dryer FL. Modeling ethylene combustion from low to high pressure. *Proceedings of the Combustion Institute* 2002; **29**:1257–1266.
33. Essenhigh RH, Mescher AM. Influence of pressure on the combustion rate of carbon. *Proceedings of the Combustion Institute* 1996; **26**:3085–3094.
34. Sivaramakrishnan R, Comandini A, Tranter RS, Brezinsky K, Davis SG, Wang H. Combustion of CO/H2 mixtures at elevated pressures. *Proceedings of the Combustion Institute* 2007; **31**(1):429–437.

DOI: 10.1002/fam